A Nonuniformly Stretched Vortex

M. Rossi,[1] F. Bottausci,[2] A. Maurel,[3] and P. Petitjeans[1]

[1]*Laboratoire de Modélisation en Mécanique, Université Pierre et Marie Curie, 4 place Jussieu, 75252 Paris, France*
[2]*Laboratoire de Physique et de Mécanique des Milieux Hétérogènes, Ecole Supérieure de Physique et de Chimie Industrielles,
10 rue Vauquelin, 75005 Paris, France*
[3]*Laboratoire Ondes et Acoustique, Ecole Supérieure de Physique et de Chimie Industrielles, 10 rue Vauquelin, 75005 Paris, France*

A stretched vortex model is proposed which includes a nonuniform stretching in the radial direction
that is clearly present in real flows, as well as a slow variation of velocity profiles along the vortex axis.
Both features of this boundary layer approximation depart from the classical Burgers solution. This
model is shown to be in very good agreement with experimental velocity measurements.

    PACS numbers: 47.32.–y, 47.15.–x

Numerical simulations [1,2] as well as real experiments [3] indicate that, in turbulent flows, vorticity is concentrated in localized regions in the form of filaments. Since strain and vorticity are dynamically coupled in the Navier-Stokes equations, it is natural to investigate how such filamentary structures undergo the action of stretching. The Burgers solution [4] $V_r = -\beta r/2$, $V_\theta = \Gamma[1 - \exp(-\nu r^2/4\beta)]/2\pi r$, $V_z = \beta z$ (V_r, V_θ, and V_z, respectively, denote the radial, azimuthal, and axial velocity component) or its asymmetric companion [5] constitute paradigmatic models for a viscous filament of circulation Γ, stretched along its axis. However, the stretching $\partial_z V_z$ of such analytical velocity fields remains radially constant, a feature which departs from what has been observed in experimental stretched filaments [6,7]. The present work defines a heuristic model including this radial dependence and a slow evolution of $\partial_z V_z$ along the vortex axis, i.e., an explicit z dependence of radial and azimuthal velocities. Both features are new and important when modeling stretched vortices in turbulent flows. Indeed, such characteristics that have been observed in experimental situations (in particular, the one presented below), may affect the vortex stability or the value of various quantities when compared to the classical Burgers case. For instance, it has been experimentally checked that the global energy balance of the stretched vortex is very much modified due to an extra energy dissipation term caused by the axial velocity shear $\partial_r V_z(r, z)$.

The theoretical model.—Let L and r_0 be the length scale of variation of the stretched vortex, respectively, along its axis and along the radial direction. The first one L is given by the global flow geometry while the second one $r_0 \equiv \sqrt{\nu/\beta}$ is determined by the balance between external stretching $\beta \equiv \partial_z V_z(r = \infty, z = 0) > 0$ and vorticity diffusion by viscosity ν. The length r_0 provides a scale for the region in which vorticity is localized (the inner region of Fig. 1). Circulation Γ is practically defined as the vorticity flux across any surface of radius much larger than r_0. In the following, spatial coordinates z and r are put in a nondimensional form using scales L and r_0, velocity components V_r, V_θ, V_z, and pressure p using, respectively, βr_0, $\Gamma/2\pi r_0$, βL, and $\rho(\Gamma/2\pi r_0)^2$. The flow is assumed to be incompressible, axisymmetric, and symmetric with respect to the stagnation point located at $(r, z) = (0, 0)$. The dynamics can then be completely written in terms of axial stretching $\gamma \equiv \partial_z V_z$ (see Fig. 1) and axial vorticity $\omega \equiv 1/r \partial_r(r V_\theta)$ since

$$V_r(r, z) = -\frac{1}{r}\int_0^r r'\gamma(r', z)\,dr',$$

$$V_\theta(r, z) = \frac{1}{r}\int_0^r r'\omega(r', z)\,dr', \qquad (1)$$

$$V_z(r, z) = \int_0^z \gamma(r, z')\,dz'.$$

Two dimensionless parameters naturally appear in the
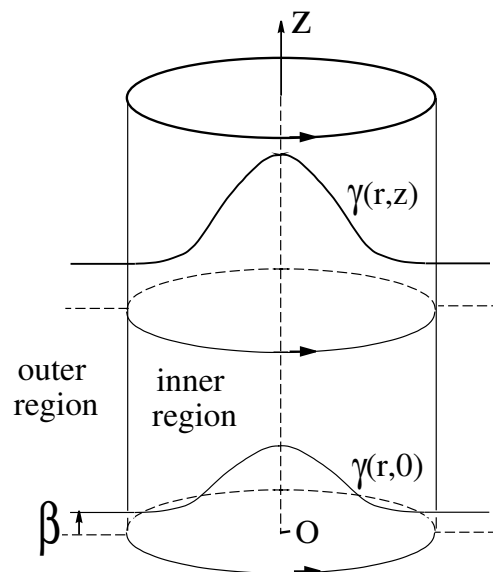
FIG. 1. Theoretical vortex model. The z axis is directed along the vortex axis and $z = 0$ defines the center of the channel and the stagnation point. $\gamma(r, z)$ denotes the axial stretching and $\beta \equiv \partial_z V_z(r = \infty, z = 0) > 0$ the external stretching at $z = 0$.

model: the inverse of a Reynolds number $\epsilon \equiv 2\pi\nu/\Gamma$ and the aspect ratio $\epsilon_1 \equiv r_0/L$. If they are both assumed small, the axisymmetric incompressible Navier-Stokes equations at leading order read as a boundary layer approximation

$$V_r\omega + V_z\partial_z V_\theta = \partial_r\omega, \tag{2}$$

$$(V_r\partial_r + V_z\partial_z)V_z = \frac{1}{r}\partial_r(r\partial_r V_z)$$
$$- T^2\partial_z\left(p(\infty, z) - \int_r^\infty \frac{V_\theta^2}{r'} dr'\right). \tag{3}$$

The term in $T^2 = (\epsilon_1/\epsilon)^2$ expresses the effect of the pressure gradient $\partial_z p(r, z)$. It is composed of the contribution of an external pressure gradient $\partial_z p(\infty, z)$ and of the centrifugal forces.

The ansatz,

$$\gamma(r, z) = \gamma^{(0)}(r) + \gamma^{(2)}(r)z^2,$$
$$\omega(r, z) = \omega^{(0)}(r) + \omega^{(2)}(r)z^2, \tag{4}$$

is proposed for systems (2) and (3). From Eq. (1), velocities V_r, V_θ should take the same polynomial form in z and velocity V_z should be of the form $az + bz^3$. This heuristic expression satisfies the symmetry with respect to the stagnation point at $z = 0$ and can be seen as a truncated Taylor expansion which contains a feature found in experimental stretched vortices: the evolution of the vortex core along the vortex axis. Within this approximation, the external pressure reads as $p(\infty, z) = -z^2/2T^2$, and stretching tends for large r (the outer region of Fig. 1) towards $\gamma(r \to \infty, z) = 1 + B/2z^2$. The term $B \equiv 2\gamma^{(2)}(\infty)$ precisely introduces the nonuniformity of stretching in the axial direction, and $\gamma^{(0)}(\infty) = 1$ by definition since the external stretching $\beta \equiv \partial_z V_z(r = \infty, z = 0) > 0$ is a scaling parameter in the nondimensionalization procedure. In the spirit of this truncated expansion, the terms in z^0, z, and z^2 are identified in systems (2) and (3) and higher orders are discarded. First, we identify the various powers of z in Eq. (2). The order z^0 provides a relation between axial vorticity $\omega^{(0)}(r)$ and stretching $\gamma^{(0)}(r)$ which can be easily solved as follows:

$$\frac{\omega^{(0)}(r)}{\omega^{(0)}(0)} = \exp\left(\int_0^r V_r^{(0)} dr'\right)$$
$$\text{with } V_r^{(j)} = -\frac{1}{r}\int_0^r r'\gamma^{(j)} dr'. \tag{5}$$

The quantity $\omega^{(0)}(0)$ is determined so that the nondimensional circulation is equal to one as imposed by our nondimensionalization procedure. The identification of power z terms in Eq. (2) is trivially satisfied and the z^2 terms lead to a second relation:

$$V_r^{(2)}\omega^{(0)} + V_r^{(0)}\omega^{(2)} + 2\gamma^{(0)}V_\theta^{(2)} = \partial_r\omega^{(2)}$$
$$\text{with } V_\theta^{(j)} = \frac{1}{r}\int_0^r r'\omega^{(j)} dr'. \tag{6}$$

Finally, let us consider the identification of powers of z in Eq. (3): The even powers z^0 and z^2 identically vanish and the z terms provide a last condition:

$$\gamma^{(0)2} - \frac{\partial_r\gamma^{(0)}}{r}\int_0^r r'\gamma^{(0)} dr' - \frac{1}{r}\partial_r(r\partial_r\gamma^{(0)}) = 1 + T^2F. \tag{7}$$

Quantity $F = 4\int_r^\infty[V_\theta^{(0)}V_\theta^{(2)}/r'] dr'$, which depends on $\gamma^{(0)}(r)$, $V_\theta^{(2)}(r)$, quantitatively expresses that the pressure gradient, generated along the axis because of the conical nature of the stretched vortex, induces an internal jet.

The system of Eqs . (5)–(7) is not closed. Such an indeterminacy is typical of boundary layer equations: It does not originate from ansatz (4) but was already present in systems (1) and (2). For instance, in a classical boundary layer flow, the streamwise velocity profile at the inflow region can be freely chosen. In the present case, one might impose a relation between $V_\theta^{(2)}(r)$ and $\gamma^{(0)}(r)$. As a first attempt, the closure $V_\theta^{(2)} = 0$ can be chosen: It actually leads to exact Navier-Stokes solutions with $V_\theta = V_\theta^{(0)}(r)$, $V_r^{(2)}(r) = 0$ [see Eq. (6)], and $B = 0$. These steady solutions have been studied in detail in [8]. However, the stretching associated with these solutions is not evolving along z, a feature not observed in our experiment. Recently, these solutions have been extended [9] to incorporate an axial velocity component independent of z or some nonaxisymmetry. However, the stretching associated with these new solutions is still not evolving along z. Moreover, except for the classical Burgers solution, such flows are characterized by a reverse axial velocity; i.e., $V_z(r)$ changes sign in $r \in [0, \infty[$ (see Appendix A). Since the experimental velocity field [7] we are considering here below has no reverse flow [Fig. 4 below], a solution with $V_\theta^{(2)} = 0$; i.e., $B = 0$ is not appropriate.

Another closure is presented for a vortex submitted to an external stretching which is nonuniform along the axial direction, i.e., $B \neq 0$. It is characterized by an azimuthal velocity depending on z and a stretching which varies in the radial direction. In that instance, radial components $V_r^{(0)}(r)$ and $V_r^{(2)}(r)$ are both non-null since, for $r \gg r_0$ (see Appendix B)

$$V_r^{(0)} \to -\frac{r}{2}, \qquad V_r^{(2)} \to -\frac{Br}{4}. \tag{8}$$

Replacing in Eq. (6) velocity components $V_r^{(0)}(r)$, $V_r^{(2)}(r)$ by their asymptotic values (8), we expect $V_\theta^{(2)}(r)$ to decrease for large r as

$$V_\theta^{(2)}(r) = \frac{B}{12}r\omega^{(0)}(r). \tag{9}$$

A possible closure consists of extending the validity of relation (9) throughout the whole r domain. This assumption satisfies as well two other requirements. First, the overall circulation remains constant along the vortex z axis since $V_\theta^{(0)} \to \frac{1}{r}$ and $V_\theta^{(2)}(r)$ is exponentially decreasing to zero for $r \to \infty$. Second, velocity $V_\theta^{(2)}$ behaves linearly

in r close to $r = 0$. Moreover, two relations follow for $V_r^{(2)}(r)$ and $\gamma^{(2)}(r)$:

$$V_r^{(2)}(r) = -\frac{B}{4} r \gamma^{(0)}(r),$$
$$\gamma^{(2)}(r) = \frac{B}{2} \gamma^{(0)}(r) + \frac{Br}{4} \frac{\partial \gamma^{(0)}}{\partial r}(r). \qquad (10)$$

Finally Eqs. (5), (7), and (9) can be written as a unique integrodifferential equation for $\gamma^{(0)}(r)$. From a given value of B, one may thus recover all other field components.

The numerical solution of this integrodifferential equation is obtained via a shooting method. The equation previously discretized by a finite difference algorithm is integrated from $r = 0$ towards $r = \infty$. Since $\frac{\partial \gamma^{(0)}}{\partial r}(r = 0)$ must be zero for obvious regularity reasons, we need to provide $\gamma^{(0)}(r = 0)$ to start the integration. The study of the asymptotic behavior of these solutions indicates that there is only one solution—hence, a unique $\gamma^{(0)}(r = 0)$—which tends for large r towards $\gamma^{(0)}(\infty) = 1$, the other solutions diverging for large r. This naturally imposes a relation between $\gamma^{(0)}(r = 0)$ and B. The shooting method is implemented so that the value of $\gamma^{(0)}(r)$ for large r is minimized with respect to the choice of $\gamma^{(0)}(r = 0)$. Moreover, the solution at $B = 0$ is known to be the classical Burgers vortex $\gamma(r) = \gamma(\infty) = 1$. By increasing step by step the value of B, we follow this unique solution.

Comparison between theoretical model and measurements—We refer here to experimental results obtained in a water channel in which a single stretched vortex is produced. The channel section is $7\,\text{cm} \times 12\,\text{cm}$. The typical longitudinal velocity is of the order of a few cm s^{-1}. A small bump added on the bottom wall (Fig. 2) induces the separation of a laminar boundary layer profile. This initial vorticity then rolls up and is strongly enhanced by stretching which is produced by sucking the flow through a hole on each lateral wall. A stretched vortex is then produced that remains attached to the suction holes (for details, see Ref. [7]). In this experiment, both assumptions of large Reynolds number and small
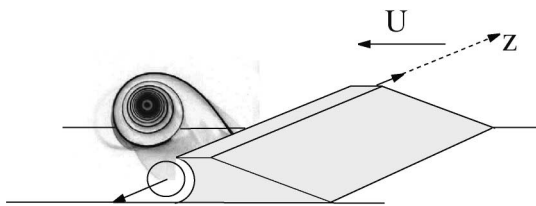
FIG. 2. Sketch of the experimental water channel. Vorticity is generated in a boundary layer which is developing over a flat plate due to the presence of a constant flow U. Such a boundary layer is then separated behind an obstacle. At the very same location, the input mass flux is entirely sucked into two tubes, each one originating from each lateral wall. Both mechanisms induce the roll-up of vorticity into a vortex structure (whose axis is along the z coordinate as in Fig. 1). A dye visualization is displayed in the inserted box.

aspect ratio are satisfied (with $\epsilon_1 = 3 \times 10^{-2} \ll 1$, $\epsilon \sim 3 \times 10^{-3} \ll 1$).

Typical azimuthal and axial velocities are, respectively, displayed in Figs. 3 and 4(a). At a fixed r location, the instantaneous velocity $V_z(r, z)$ is fitted with a polynomial of the form $\gamma_{\exp}^{(0)} z + \gamma_{\exp}^{(2)} z^3/3$ [as assumed by Eqs. (1) and (4)]. Since this is performed for each r, the profiles $\gamma_{\exp}^{(0)}(r)$ and $\gamma_{\exp}^{(2)}(r)$ are obtained from the experimental measurements of $V_z(r, z)$. Results are shown in Figs. 4(b) and 4(d). Note that the obtained V_z profiles are smoothed also in the radial direction although the fits were performed in the z direction. The discrepancy $\overline{\Delta V_z / V_z}$ (overbars indicate that mean values are taken over the whole r and z domain) measures the difference between the experimental data and the fit $\Delta V_z = V_z(r, z) - [\gamma_{\exp}^{(0)}(r) z + \gamma_{\exp}^{(2)}(r) z^3/3]$. It is of the order of 10%.

In our theoretical model, B is the only free parameter. It is fixed so that $\gamma^{(0)}(0)$ is similar to the experimental value. The theoretical stretching $\gamma^{(0)}(r)$, obtained by integrating the integrodifferential equation, nicely compares with the experimental one [see Fig. 4(d)]. Similarly, comparisons first between the theoretical solutions $V_\theta(r, z) = V_\theta^{(0)}(r) + z^2 V_\theta^{(2)}(r)$ and the experimental profiles (presented in Fig. 3) and, second, between the theoretical solution $V_z(r, z) = \gamma^{(0)} z + \gamma^{(2)} z^3/3$ and the experimental field [presented in Figs. 4(a) and 4(c)] both show a very satisfactory agreement.

Conclusion—The proposed model, based on a boundary layer approximation, is clearly closer to a real stretched vortex, e.g., those found in turbulent flows, than the classical Burgers vortex, particularly regarding the localization of stretching in the vortex core. It seems
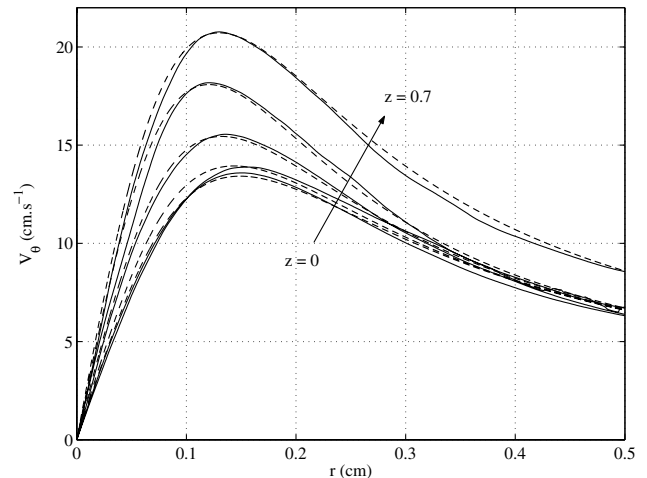
FIG. 3. In plain lines, V_θ profiles [averaged particle image velocimetry (PIV) measurements] for nondimensional $z = 0$, 0.17, 0.3, 0.5 ($L = 6$ cm, imposed by the channel width) and $z = 0.7$ ($L = 3$ cm when reducing the channel width). In dotted lines, corresponding theoretical solutions $V_\theta(r, z) = V_\theta^{(0)}(r) + V_\theta^{(2)}(r) z^2$ ($B = 1.6$ for $L = 3$ cm and $B = 11.5$ for $L = 6$ cm).
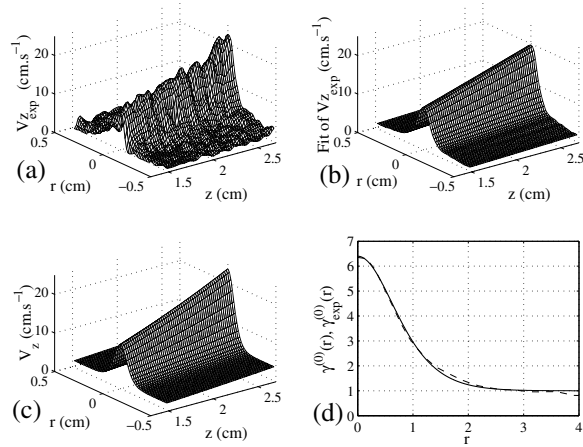
FIG. 4. (a) $V_z(r, z)$ field (instantaneous PIV measurement) for $L = 3$ cm. (b) Fit of the previous field in $\gamma_{\exp}^{(0)}(r)z + \gamma_{\exp}^{(2)}(r)z^3/3$ performed at each r. (c) Theoretical field $V_z(r, z) = \gamma^{(0)}(r)z + \gamma^{(2)}(r)z^3/3$. (d) Comparison between $\gamma_{\exp}^{(0)}(r)$ and $\gamma^{(0)}(r)$ [$\gamma_{\exp}^{(2)}(r)$, being of the same order of the noise, is not displayed].

worthwhile to study the stability of the present vortex model in relation to the scenario of transition to turbulence proposed in [11] via primary and secondary instabilities of an elliptic vortex.

Appendix A: Uniform stretching along the axis, $B = 0$—. If $B = 0$, the solution is characterized by a constant core size along the vortex axis and an azimuthal velocity V_θ independent of the position z. Moreover, stretching $\gamma = \gamma^{(0)}(r)$ satisfies the dimensionless integro-differential equation

$$\gamma^{(0)2} - \frac{\partial_r \gamma^{(0)}}{r}\left(1 + \int_0^r r'\gamma^{(0)}dr'\right) - \partial_{r^2}\gamma^{(0)} = 1. \quad (A1)$$

The above solutions have been studied in detail in [8]. For such cases, let us show that, on a general basis, stretching or, equivalently, axial velocity $V_z(r, z) = \gamma(r)z$ are bound to change sign in $r \in [0, \infty]$. Assuming this is not the case, two possibilities then arise: (a) $1 < \gamma(0)$ or else (b) $0 < \gamma(0) < 1$ [$\gamma(0) = 1$ corresponds to the Burgers solution]. Equation (A1) at $r = 0$ shows that $2\partial^2\gamma/\partial r^2(0) = \gamma^2(0) - 1$. In the first instance (a), stretching $\gamma(r)$ starts to increase as r increases near $r = 0$. This quantity cannot decrease afterwards in $[0, \infty]$: otherwise, a point $r_d > 0$ would exist such that

$$\begin{aligned}\frac{\partial\gamma}{\partial r}(r_d) = 0; \qquad \gamma(r_d) > \gamma(0) > 1, \\ \text{and} \quad \frac{\partial^2\gamma}{\partial r^2}(r_d) = \gamma^2(r_d) - 1 < 0.\end{aligned} \quad (A2)$$

This inequality being clearly inconsistent, $\gamma(r)$ is then always greater than $\gamma(0) > 1$ and cannot reach one at $r = \infty$. If one assumes case (b) to be valid, stretching $\gamma(r)$ always decreases in the interval $\gamma(r) \in [0, 1]$ for similar

reasons. As a consequence, it cannot reach one at $r = \infty$ without changing sign.

Appendix B: Boundary conditions for case $B \neq 0$—. The solution presented in the main body of the paper is typically focusing on the region close to the vortex which scales with r_0 (the inner region of Fig. 1). More precisely, systems (2) and (3) constitute the leading order approximation in this zone [11]. Within the asymptotic expansion theory, this inner region is associated to an outer region and the expressions of the solution in the two regions should match. In the present case, the outer region is located away from the vortex, i.e., in a region which scales in the radial direction with L. The vortex being surrounded by an irrotational field, the leading order outer expansion is thus characterized by a potential velocity field $V_r = \partial_r\psi$, $V_z = \partial_z\psi$, with $\Delta\psi = 0$. The matching principle states (see Ref. [12] for a presentation of the asymptotic matching principles) that the leading order inner solution for $r \gg r_0$ matches the leading order outer solution for $r \to 0$. For $r \to 0$, the potential defining the outer field generally reads as $\psi(r, z) = \phi_0(z) + \partial_z^2\phi_0(z)r^2/4 + \cdots$. As a consequence, the outer vortex field should be of the form

$$V_r \to -\frac{r}{2}\partial_z^2\phi_0(z), \qquad V_z \to \partial_z\phi_0(z). \quad (B1)$$

To match the inner solution $\gamma(r)$ at $r \to \infty$, i.e., $\gamma(r) = 1 + \frac{B}{2}z^2$ to the outer field at $r \to 0$, one must choose $\phi_0(z) = (z^2/2) + \frac{B}{24}z^4$ which provides the conditions

$$V_r^{(0)} \to -\frac{r}{2}, \qquad V_r^{(2)} \to -\frac{Br}{4}. \quad (B2)$$

[1] E. D. Siggia, J. Fluid Mech. **107**, 37 (1981).
[2] A. Vincent and M. Meneguzzi, J. Fluid Mech. **225**, 1 (1991).
[3] O. Cadot, D. Douady, and Y. Couder, Phys. Fluids **7**, 630 (1995).
[4] P. G. Saffman, *Vortex Dynamics* (Cambridge University Press, Cambridge, England, 1992).
[5] H. K. Moffatt, S. Kida, and K. Ohkitani, J. Fluid Mech. **259**, 241 (1994).
[6] B. Andreotti, S. Douady, and Y. Couder, J. Fluid Mech. **444**, 151 (2001).
[7] P. Petitjeans, J. H. Robres, J. E. Wesfreid, and N. Kevlahan, Eur. J. Mech. B/Fluids **17**, 549 (1998).
[8] R. D. Sullivan, J. Aerospace Sci. **26**, 26 (1959).
[9] J. D. Gibbon, A. S. Fokas, and C. R. Doering, Physica (Amsterdam) **132D**, 497 (1999).
[10] T. S. Lundgren and N. N. Mansour, J. Fluid Mech. **307**, 43 (1996).
[11] J. Kervorkian and J. D. Cole, *Perturbations Methods in Applied Mathematics* (Springer, New York, 1981).